

Uncertainty quantification of receptor ligand binding sites prediction

Nanjie Chen, Dongliang Yu, Dmitri Beglov, Mark Kon, Julio Enrique Castrillón-Candás

Abstract—Recent advancements in protein docking site prediction have highlighted the limitations of traditional rigid docking algorithms, like PIPER, which often neglect critical stochastic elements such as solvent-induced fluctuations. These oversights can lead to inaccuracies in identifying viable docking sites due to the complexity of high-dimensional, stochastic energy manifolds with low regularity. To address this issue, our research introduces a novel model where the molecular shapes of ligands and receptors are represented using multi-variate Karhunen-Loève (KL) expansions. This method effectively captures the stochastic nature of energy manifolds, allowing for a more accurate representation of molecular interactions. Developed as a plugin for PIPER, our scientific computing software enhances the platform, delivering robust uncertainty measures for the energy manifolds of ranked binding sites. Our results demonstrate that top-ranked binding sites, characterized by lower uncertainty in the stochastic energy manifold, align closely with actual docking sites. Conversely, sites with higher uncertainty correlate with less optimal docking positions. This distinction not only validates our approach but also sets a new standard in protein docking predictions, offering substantial implications for future molecular interaction research and drug development.

Index Terms—Karhunen-Loeve Expansion, Proper Orthogonal Decomposition, Stochastic Modeling, Uncertainty Quantification



1 INTRODUCTION

THE exploration of protein docking and broader molecular interactions has become a significant focus within the field of biology. In fact, computational approaches have already demonstrated success in identifying potential compounds for the treatment of novel diseases, thereby expediting the drug design process. This is especially relevant and vital considering the recent global health crises triggered by pandemics.

A popular computational approach for predicting receptor-ligand binding sites is known as rigid body docking, where the molecular shapes are assumed to be fixed (Piper [1], ZDock [2], FFT, FMFT [3], etc). While this method is computationally efficient, rigid docking can fail to accurately predict the binding site if: i) Either the shape of the receptor or ligand varies significantly during the binding process. ii) The conformational shape of the receptor or ligand is uncertain due to the kinetic presence of the solvent atoms. To address the latter, flexible Docking was developed [4]. In contrast to rigid docking method, where both receptor and ligand are treated as rigid bodies, flexible docking acknowledges the potential conformational molecular changes that can occur during the binding process. While this approach can yield a more accurate prediction, it simultaneously intensifies computational complexity. And the accuracy of flexible docking is greatly dependent on

the modeling of the protein and ligand’s flexibility, as well as the initial state or conformation of the molecules [5][6]. Furthermore, the flexible docking method tackles conformational changes by integrating molecular flexibility in a deterministic manner. [7].

However, to address ii), considering the thermal random fluctuations that originate from the solvent, it becomes more practical to incorporate conformational uncertainty as random fields. This necessitates the development of a docking method that more realistically models receptor-ligand binding sites under conformational uncertainty, balancing both accuracy and efficiency. In this paper, we introduce a stochastic framework for assessing the inherent uncertainty in rigid docking. Our future work will strive to extend this methodology to encompass other docking methods.

Computational receptor-ligand interactions (Docking calculations) involve two methodological selections. The first involves a goodness of fit, sometimes called a scoring function, which assigns a numerical quality measure to each configuration of the two bodies. This in turn defines an energy manifold parametrized by the molecular spatial degrees of freedom, on which the optimal binding site is sought. The second selection involves the choice of search algorithm on the energy manifold. Both of these choices are based on some assumed molecular model. The partially heuristic scoring function incorporates various aspects of molecular properties, including electron density representations of the molecular shape, electrostatic (see Figure 1 for an example of potential fields for the Trypsin protein) and solvation terms [8, 9] and structure-based interaction potentials [1, 10].

One popular approach to rigid docking is based on Fast Fourier Transforms (FFTs). The mathematical formulation of this method is formulated as follows. Let $\mathbf{x} := [x, y, z]^T \in \mathbb{R}^3$ be spatial coordinates, $\boldsymbol{\alpha} := [\alpha, \beta, \lambda]^T \in \mathbb{R}^3$ be the

N.Chen is with Graduate School of Mathematics and Statistics, Boston University, Boston, USA

D.Yu is with Graduate School of Mathematics, Stony Brook University, Stony Brook, USA

D.Beglov is with the Faculty of Biomedical Engineering, Boston University, Boston, USA.

M.Kon is with the Faculty of Mathematics and Statistics, Boston University, Boston, USA

J.Castrillón-Candás is with the Faculty of Mathematics and Statistics, Boston University, Boston, USA

rotational coordinates, and $\mathbf{v} = [\lambda, \mu, \nu]^T \in \mathbb{R}^3$ be the translational coordinates. For $p = 1, \dots, P$, let $L_p(\mathbf{x}) : \mathbb{R}^3 \rightarrow \mathbb{C}$, $R_p(\mathbf{x}) : \mathbb{R}^3 \rightarrow \mathbb{C}$ be respectively the different ligand and receptor molecular property maps. The scoring energy function of the receptor-ligand interaction is given by:

$$E(\boldsymbol{\alpha}, \boldsymbol{\lambda}) := \sum_{k=1}^P \int_{\mathbb{R}^3} \overline{R_k(\mathbf{x})} (T(\boldsymbol{\lambda})D(\boldsymbol{\alpha})L_k(\mathbf{x})) d\mathbf{x}$$

where $T : \mathbb{R}^3 \rightarrow \mathbb{R}^3$ is the translation operator, $D : \mathbb{R}^3 \rightarrow \mathbb{R}^3$ is the rotation operator. Our goal is to obtain the optimal docking site by searching the six dimensional function $E(\boldsymbol{\alpha}, \boldsymbol{\lambda})$ for the minimal energy, that is, finding the docking site $(\boldsymbol{\alpha}_{bind}, \boldsymbol{\lambda}_{bind})$ such that $E(\boldsymbol{\alpha}, \boldsymbol{\lambda})$ is minimized.

The key weakness of rigid docking is that the geometry of the molecule is assumed to be deterministic and fixed. Indeed only the crystal structure in many cases is known (Protein Data Bank [11]). However, uncertainty in the molecular shape can lead to a predicted erroneous docking site. The *true* molecular conformation can in fact involve significantly different docking sites. In particular thermal fluctuations and solvent interactions among other factors lead to different conformations of the protein. In [12, 13] molecular dynamics are used to describe particle movements, using stochastic initial velocities. Nonetheless, this model assumes that the particles are contained in a vacuum, while interactions with the solvent are ignored. In contrast, NAMD is a popular molecular dynamic software for simulating molecular dynamics in a solvent [14]. Other approaches to molecular dynamics are based on Langevin dynamics [15–17] and Markov random models [18].

Due to the random fluctuations of the protein in the solvent, the molecular shape becomes stochastic. Let Ω denote the set of all possible outcomes in a complete probability space $(\Omega, \mathcal{F}, \mathbb{P})$, with \mathcal{F} a σ -algebra of events and \mathbb{P} the probability measure. Given dynamic thermal randomness and the resulting conformational uncertainties, the receptor and ligand molecular maps will now depend on a random parameter $\omega \in \Omega$ i.e. for $k = 1, \dots, P$ we have $R_k(\mathbf{x}, \omega) : \mathbb{R}^3 \times \Omega \rightarrow \mathbb{C}$ and $L_k(\mathbf{x}, \omega) : \mathbb{R}^3 \times \Omega \rightarrow \mathbb{C}$ and the energy function can be expressed as

$$E(\boldsymbol{\alpha}, \boldsymbol{\lambda}, \omega) := \sum_{k=1}^P \int_{\mathbb{R}^3} \overline{R_k(\mathbf{x}, \omega)} T(\boldsymbol{\lambda})D(\boldsymbol{\alpha})L_k(\mathbf{x}, \omega) d\mathbf{x}.$$

We develop a framework to quantify the uncertainty of proposed binding sites given a stochastic manifold representation of the shape of the receptor and ligand in a solvent. This approach originates from the fields of scientific computing, and numerical analysis. More precisely, these tools are adopted from uncertainty quantification to assess the fitness of the proposed *rigid body* docking site. To facilitate this process, we have developed a software tool that serves as a wrapper (plugin) for PIPER [1], enabling the quantification of uncertainty in the predicted rigid body docking site. With the application of Karhunen-Loeve Theorem on conformational molecular shape, we confirm the existence of a stochastic manifold representation of a conformational shape as an infinite linear combination of orthonormal functions with stochastic coefficients. This expansion is optimal compared to all other orthogonal representations

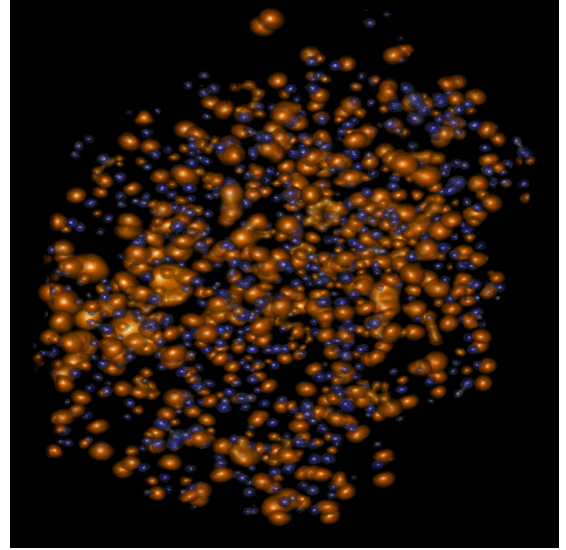


Figure 1: Non-linear electrostatic potential of Trypsin (PDB 1PPE). The potential fields were created with APBS [19] rendered with VolRover [20, 21]. The positive and negative potential are rendered with blueish and orange/reddish colors respectively.

in the sense of minimizing mean square error. A detailed discussion on the Karhunen-Loeve Theorem, essential for comprehending the functionality of our stochastic framework, is available in the subsequent section."

2 MATHEMATICAL BACKGROUND

2.1 Karhunen-Loeve Theorem

Due to the stochastic nature of the interactions between the solvent and the protein, we model the uncertainty in the molecular shape as a random field (stochastic process). This representation is infinite dimensional thus motivating the construction of accurate finite dimensional noise models. The KL theorem provides an optimal finite dimensional model in a stochastic norm sense. Karhunen-Loeve Theorem has been extensively used in model reduction, data analysis, signal processing, and many other fields. It is also known as proper orthogonal decomposition, singular value decomposition, functional principal components.

Let D be a subset in \mathbb{R}^d . Define $L^2(D; \mathbb{R}^q)$ to be a Hilbert space which consists of all the square integrable functions from D to \mathbb{R}^q equipped with the inner product $(\cdot, \cdot)_{L^2(D; \mathbb{R}^q)}$ defined as $(f, g)_{L^2(D; \mathbb{R}^q)} := \int_D f^T g dx$ for all $g, f \in L^2(D; \mathbb{R}^q)$. Let $(\Omega, \mathcal{F}, \mathbb{P})$ be a complete probability space, where Ω is the set of outcomes, \mathcal{F} is the sigma algebra of events, and \mathbb{P} is the associated probability measure. Consider the random vector field $u : \Omega \rightarrow L^2(D; \mathbb{R}^q)$. We define a suitable Hilbert space that incorporates the spatial and probability components. To this end, let $L^2_{\mathbb{P}}(\Omega; L^2(D; \mathbb{R}^q))$ be a Bochner space that is equipped with the inner product $(\cdot, \cdot)_{L^2_{\mathbb{P}}(\Omega; L^2(D; \mathbb{R}^q))}$ such that for all $w, v \in L^2_{\mathbb{P}}(\Omega; L^2(D; \mathbb{R}^q))$ we have that

$$(w, v)_{L^2(\Omega; L^2(D; \mathbb{R}^q))} := \mathbb{E}[(w, v)] := \int_{\Omega} (w, v) d\mathbb{P}.$$

Note that the corresponding norm $\|v\|_{L^2_{\mathbb{P}}(\Omega; L^2(D; \mathbb{R}^q))}$ for all $v \in L^2(\Omega; L^2(D; \mathbb{R}^q))$ of the Bochner space is defined as

$$\|v\|_{L^2(\Omega; L^2(D; \mathbb{R}^d))} := (v, v)_{L^2(\Omega; L^2(D; \mathbb{R}^q))}^{\frac{1}{2}}.$$

Remark 1. The definition of the Bochner space might appear somewhat abstract. However, this space will be important since we assume that the random fluctuations of the molecule shape are described by a random vector field $u \in L^2(\Omega; L^2(D; \mathbb{R}^q))$. This space allow us to construct finite dimensional representations of the random fluctuations of the protein by using KL expansions.

Definition 1.

- 1) For all $u(\mathbf{v}) \in L^2(\Omega; L^2(D; \mathbb{R}^q))$, where $u(\mathbf{v}) := [u_1(\mathbf{v}, \omega), u_2(\mathbf{v}, \omega), \dots, u_d(\mathbf{v}, \omega)]$ let

$$\mathbb{E}[u_i(\mathbf{v}, \omega)] := \int_{\Omega} u_i(\mathbf{v}, \omega) d\mathbb{P},$$

for $i = 1, 2, \dots, d$.

- 2) For all $u \in L^2(\Omega; L^2(D; \mathbb{R}^q))$,

$$\text{Cov}(u_i(\mathbf{v}), u_j(\mathbf{y})) := \mathbb{E}[(u_i(\mathbf{v}) - \mathbb{E}[u_i(\mathbf{v})]) (u_j(\mathbf{y}) - \mathbb{E}[u_j(\mathbf{y})])]$$

for $i, j = 1, \dots, d$. Denote the covariance matrix function of u between index \mathbf{v} and index \mathbf{y} as

$$R_u(\mathbf{v}, \mathbf{y}) := \text{Cov}(\mathbf{u}(\mathbf{v}), \mathbf{u}(\mathbf{y})) \quad (1)$$

- 3) Associate to R_u a linear operator T_{R_u} defined in the following way:

$$T_{R_u} : L^2(D) \rightarrow L^2(D) : f \rightarrow T_{R_u} f = \int_D R_u(\mathbf{s}, \cdot) f(\mathbf{s}) d\mathbf{s} \quad (2)$$

$$\int_D R_u(\mathbf{s}, \mathbf{v}) \phi_k(\mathbf{s}) d\mathbf{s} = \lambda_k \phi_k(\mathbf{v}) \quad (3)$$

where $\{\phi_k, k \in \mathbb{N}\}$ are orthonormal eigenfunctions of T_{R_u} in $L^2(D)$ with respect to eigenvalues $\{\lambda_k, k \in \mathbb{N}\}$.

The following theorem shows that any random field $u \in L^2_{\mathbb{P}}(\Omega, L^2(D, \mathbb{R}^q))$ can be represented as an infinite sum in terms of eigenvalues, eigenfunctions ($\{(\lambda_k, \phi_k)\}_{k \in \mathbb{N}}$) and random components.

Theorem 1 (Multivariate Karhunen-Loeve expansion). Let $u(\mathbf{v}, \omega)$ be a zero mean vector process in $L^2(\Omega; L^2(D; \mathbb{R}^q))$, then $u(\mathbf{v})$ admits the following representation:

$$u(\mathbf{v}, \omega) = \sum_{k=1}^{\infty} Z_k(\omega) \phi_k(\mathbf{v}) \quad (4)$$

where the convergence is in $\|\cdot\|_{L^2_{\mathbb{P}}(\Omega; L^2(D; \mathbb{R}^q))}$, and

$$Z_k(\omega) = \int_D u(\mathbf{v}, \omega)^T \phi_k(\mathbf{v}) d\mathbf{v} \quad (5)$$

Furthermore, Z_k are uncorrelated with mean zero and variance λ_k .

Remark 2. The general case of a process $u_{\mathbf{v}}$ that is not centered can be brought back to the case of a centered process by considering $u_{\mathbf{v}} - \mathbb{E}(u_{\mathbf{v}})$, which is a centered process.

A key feature of the KL Theorem is that the truncated expansion is optimal in the sense that among all finite di-

dimensional orthonormal basis approximations it minimizes the total mean square error.

Proposition 1. Let $\mathcal{B} = \{\psi_i(\mathbf{v}, \omega)\}_{i \in \mathbb{N}}$ be a complete orthonormal basis of $L^2_{\mathbb{P}}(\Omega; L^2(D; \mathbb{R}^d))$, and $\mathcal{B}^p = \{\psi_i(\mathbf{v}, \omega)\}_{i=1, \dots, p}$ be a collection of p basis functions in \mathcal{B} . Let \tilde{u}_p be the orthogonal projection of $u(\mathbf{v}, \omega)$ (approximation) onto the finite dimensional subspace with the following orthonormal basis functions, e.g.

$$\tilde{u}_p(\mathbf{v}, \omega) = \sum_{i=1}^p \left(\int_D \int_{\Omega} u(\mathbf{v}, \omega) \psi_i(\mathbf{v}, \omega) d\mathbf{v} d\mathbb{P} \right) \psi_i(\mathbf{v}, \omega)$$

Denote \mathcal{C} to be the set of all complete orthonormal bases of $L^2_{\mathbb{P}}(\Omega; L^2(D; \mathbb{R}^d))$. For any basis $\tilde{\mathcal{B}} \in \mathcal{C}$ let $\tilde{\mathcal{B}}^p$ be the collection of any p basis functions in $\tilde{\mathcal{B}}$ and

$$\mathcal{C}^p = \{\tilde{\mathcal{B}}^p \mid \tilde{\mathcal{B}} \in \mathcal{C}\}.$$

Then

$$\underset{\mathcal{C}^p}{\text{arginf}} \int_D \mathbb{E}[Err_p^2(\mathbf{v})] d\mathbf{v} = \left\{ \frac{\phi_1(\mathbf{v}) Z_1(\omega)}{\sqrt{\lambda_1}}, \frac{\phi_2(\mathbf{v}) Z_2(\omega)}{\sqrt{\lambda_2}}, \dots, \frac{\phi_p(\mathbf{v}) Z_p(\omega)}{\sqrt{\lambda_p}} \right\}$$

where

$$Err_p(\mathbf{v}) := u - \tilde{u}_p = \sum_{i \geq p+1} \alpha_i \psi_i(\mathbf{v}, \omega),$$

where

$$\alpha_i = \int_D \int_{\Omega} u(\mathbf{v}, \omega) \psi_i(\mathbf{v}, \omega) d\mathbf{v} d\mathbb{P}$$

for $i \geq p + 1$.

Remark 3. To apply Karhunen Loeve expansion, we only need to have eigenfunctions ϕ_k and random coefficient Z_k . It is not hard to obtain the former as long as we can construct a covariance matrix based on data and apply the method of snapshot [22] to estimate eigenfunction empirically. However, it can be infeasible to estimate the true probability distribution of the random field and hence the true random coefficients Z_k due to high dimensions, especially in general, Z_k are only uncorrelated rather than independent.

Remark 4. In practice, the Karhunen-Loeve expansion is truncated to a finite number of terms. Consider a $d \times d$ covariance matrix, where d denotes the dimension of the feature. High dimensional features can lead to large covariance matrices, where solving the eigenvalue decomposition problem may be infeasible. The snapshot method derived by Sirovich [22] can potentially reduce the high dimensional problem of solving eigenfunctions for a continuous covariance function $R_u(\mathbf{s}, \mathbf{v})$ to an eigenvalue decomposition problem of a finite-dimensional matrix by taking snapshots (samples) at discrete times, where the number of snapshots is usually much smaller than dimension d , hence makes the eigen decomposition problem more affordable (See Appendix A for more details).

It can be shown that Karhunen Loeve expansion preserves the covariance structure of observations no matter what distribution the random coefficients follow.

Proposition 2. Assume that $\tilde{Z}_k(\omega)$ for all $k \in \mathbb{N}$ are orthonormal in $L^2(\Omega; L^2(D; \mathbb{R}^q))$ of zero mean, variance λ_k . The

Karhunen Loeve expansion of zero mean vector process $u(\mathbf{v})$ with \tilde{Z}_k as random coefficients will be:

$$\tilde{u}(\mathbf{v}, \omega) = \sum_{k \in \mathbb{N}} \phi_k(\mathbf{v}) \tilde{Z}_k(\omega)$$

The covariance function $\text{Cov}(\tilde{v}(\mathbf{x}, \omega), \tilde{v}(\mathbf{y}, \omega)) = \sum_{k \in \mathbb{N}} \lambda_k \phi_k(\mathbf{x}) \phi_k(\mathbf{y}) = \text{Cov}(v(\mathbf{x}, \omega), v(\mathbf{y}, \omega))$. In other words, no matter what distribution \tilde{Z}_k follows, the covariance function of the new random field formed based on these random coefficients will be the same as the true one.

Furthermore, if the random field is Gaussian, random coefficients Z_k are not just uncorrelated.

Proposition 3. *If the process $u(\mathbf{v}) \in L^2(\Omega : L^2(D; \mathbb{R}^d))$ is Gaussian, then the random variables $Z_k \sim \mathcal{N}(0, \lambda_k)$ are normal and identically independent distributed.*

Consequently, we can assume that the random vector field $u(\mathbf{v}, \omega)$ follows a Gaussian distribution, thereby rendering the random coefficients independent. As already demonstrated in Proposition 2, regardless of the distribution assigned to the stochastic manifold, the covariance structure for atomic coordinates remains consistent. This consistency is ensured by Mercer's theorem, which affirms that a symmetric, positive-definite matrix can be uniquely expressed as a sum of a convergent sequence, composed solely of eigenvalues and eigenfunctions (as demonstrated in Appendix, equation (A.1)). This representation thus retains the original molecular structural information [23].

Remark 5. *For reasons of generality, the probability spaces that are defined with respect to an extensive set of outcomes Ω . However, under certain conditions, the probability measure $\mathbb{P} : \Omega \rightarrow \mathbb{R}^+$ can be associated with the probability density function $\varrho(\mathbf{x}) : \mathbb{R}^q \rightarrow \mathbb{R}^+$, for some $q > 0$ [24]. Let $\mathbf{z} = (z_1(\omega), z_2(\omega), \dots, z_q(\omega))$ be a q -valued random vector where each random variable $z_k(\omega)$ is defined as in Theorem 1. Note that the random vector \mathbf{z} is a function from Ω to \mathbb{R}^q . This gives us the more familiar form of expectation:*

$$\mathbb{E}(u(\mathbf{v}, \omega)) := \int_{\Omega} u(\mathbf{v}, \omega) d\mathbb{P} = \int_{\mathbb{R}^q} u(\mathbf{v}, \mathbf{z}) \varrho(\mathbf{z}) d\mathbf{z}.$$

By our assumption, the probability density function ϱ is known to be the Gaussian probability density function. For convenience, in the subsequent sections, we will replace all ω with $\mathbf{z}(\omega)$.

3 PROBLEM FORMATION

3.1 Protein Stochastic Model

The uncertainties in the molecular conformation can be propagated to the receptor and ligand molecular maps and eventually to the energy function as

$$\mathbb{E}(\alpha, \lambda, \omega) := \sum_{p=1}^P \int_{\mathbb{R}^3} \overline{R_p(\mathbf{x}, \omega)} T(\lambda) D(\alpha) L_p(\mathbf{x}, \omega) d\mathbf{x}$$

We further compute the mean log of the energy function $\mathbb{E}[\log E(\alpha, \lambda, \omega)]$ for smoothing. Our goal is to choose the docking site (α, λ) such that the mean log is minimized by computing $\text{argmin}_{\alpha, \lambda} \mathbb{E}[\log E(\alpha, \lambda, \omega)]$. "Nevertheless, a

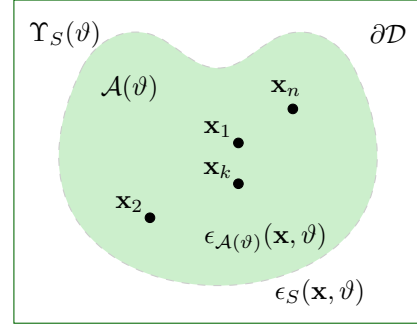


Figure 2: Two dimensional representation of receptor and solvent.

significant standard deviation implies a considerable fluctuation in the energy function with respect to the random conformation. Under such circumstances, it may be more suitable to identify potential candidates for the docking site. (α, λ) which has both small mean and standard deviation by computing $\mathbb{E}[\log(E(\alpha, \lambda, \omega) + \delta)]$ and $\text{SD}[\log E(\alpha, \lambda, \omega) + \delta]$ for some user-given parameter $\delta > 0$ chosen such that $E(\alpha, \lambda, \omega) + \delta > 1$. This will enable us to construct a stochastic framework for decision making to determine the uncertainty of a docking site by its mean and standard variance of energy.

For many cases, for each rotational and translational search (α, λ) the function $E(\alpha, \lambda, \omega)$ is a high dimensional, non-Gaussian and non-linear random field with respect to the stochastic parameter ω . Each rotational and translational configuration (α, λ) will correspond to computing the mean and SD of the high dimensional function $\log(E(\alpha, \lambda, \omega) + \delta)$. However, it is a daunting task to compute the expectation and standard deviation of each docking site. Suppose that $E(\alpha, \lambda, \omega) : \Omega \rightarrow \mathbb{R}^6$ is modeled with N stochastic dimensions. Thus the total number of dimensions of the domain of $E(\alpha, \lambda, \omega) : \mathbb{R}^6 \times \Omega \rightarrow \mathbb{R}$ will correspond to 3 translations and 3 rotational dimensions plus N stochastic dimensions. Then for even a relatively small number of dimensions N , the stochastic optimization will become intractable. In contrast, given the sparse grid approximation the optimization objective function is approximated with a surrogate model and the problem reduces to

$$(\lambda^*, \alpha^*) := \text{argmin}_{\alpha, \lambda} (\mathbb{E}[\log(E(\alpha, \lambda, \omega) + \delta)] + \beta \text{SD}[\log E(\alpha, \lambda, \omega)]) . \quad (6)$$

The integration can be computed by using the Sparse Grid Radial Basis function discussed below.

Even without high regularity of the molecular maps with respect to the random variables, the expected value and standard deviation of each docking site can be computed accurately with just a relatively few realizations of the stochastic domains of locations of protein molecules. Once the optimal docking site (λ^*, α^*) is obtained we have indeed also estimated the mean and std of $E(\alpha, \lambda, \omega)$. These estimates also provides us statistical information on suitability of the docking site. The mean and second moment of

energy are defined as:

$$\begin{aligned} & \mathbb{E} [\log(E(\alpha, \lambda, \omega) + \delta)] \\ &= \int_{\Omega} \log(E(\alpha, \lambda, \omega) + \delta) \rho(\omega) d\omega \end{aligned} \quad (7)$$

and

$$\begin{aligned} & \mathbb{E} \left[(\log(E(\alpha, \lambda, \omega) + \delta))^2 \right] \\ &= \int_{\Omega} (\log(E(\alpha, \lambda, \omega) + \delta))^2 \rho(\omega) d\omega \end{aligned} \quad (8)$$

We follow an uncertainty decision tree to filter out configurations of high uncertainty which are unlikely to be the true docking site. This process is based on determining the level of uncertainty by comparing mean and variance. The configuration of rotation and transition which has low mean and variance can be considered as the one of low uncertainty, and hence a good and more likely candidate, and if either of the mean or variance is high, the configuration is of high uncertainty and low likelihood of being the docking site. More details are shown in Figure 3. The decision tree can provide a list of reasonable candidates of docking site by removing those impossible configurations of high uncertainty.

Remark 6. Note that, due to local low regularity and high dimensions, it is computationally difficult to capture all the uncertainty on the stochastic molecular manifold, but finding the sites of extremely high uncertainty is still feasible by calculating mean and variance of energy. If mean and variance indicate high uncertainty, then this result is of high confidence; however if mean and variance are both low, at the current stage that doesn't guarantee the corresponding configuration is of low uncertainty due to the computational inaccuracy because of truncation error and integration error. For more details about the errors and difficulties this framework and decision making process have to undergo, please read the Discussion section 5.

Remark 7. Criterion for mean and variance of energies, C_{μ} and C_{σ^2} , have to be set to determine whether a configuration has high uncertainty or not. One way is choosing high quantile (e.g. 0.8) of empirical distribution of energy means and variances as criterions respectively.

3.2 The approach

In this section, we will show the general process of constructing the stochastic framework of molecular dynamic manifold. Assume that the conformation manifold of receptor or ligand is a Gaussian random field, and truncate the Gaussian random field by drawing a circle centered at mean with a radius of three standard deviations. It is to be observed that the covariance structure under this assumption will be identical to the true one since the covariance function (kernel) can be expressed as the sum of convergent sequence in terms of eigenfunctions and corresponding eigenvalues by the Mercer's theorem.

The first step is applying the Karhunen-Loeve expansion we introduced above on the atom coordinates of receptor/ligand to obtain the stochastic atom coordinates. Let

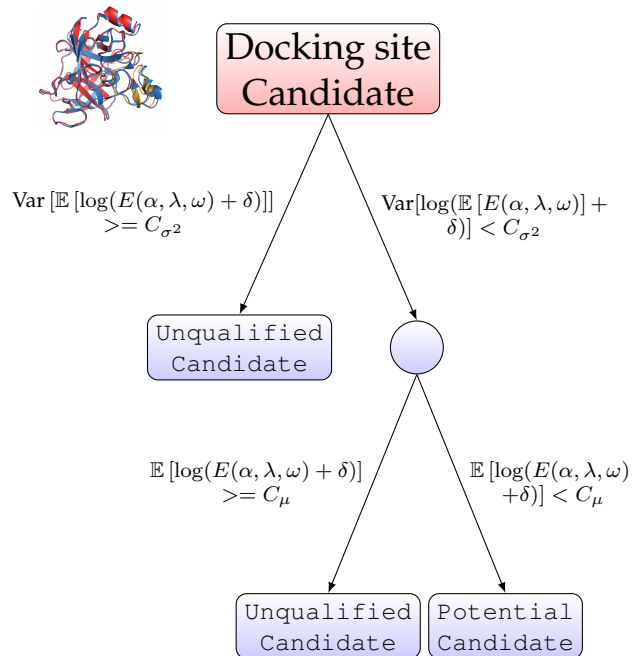


Figure 3: Docking candidate decision tree process: Step 1: Compare the variance of energy, if variance is greater than the criterion C_{σ^2} set beforehand, then the corresponding configuration is determined to be of high uncertainty, and should be filtered out. Step 2: For the remaining configurations of variance smaller than criterion for variance, abandon the ones whose mean of energy is greater than C_{μ} , the criterion for mean, keep the ones whose mean is smaller than C_{μ} . By removing those configurations which already be determined as impossible candidates, the final result obtained is a list of potential candidates which is awaited for further study in higher dimensional stochastic molecular conformational space to find the optimal docking site.

$u_R = [x_R, y_R, z_R]$ be a $M_R \times 3$ matrices where each row is the 3-dimensional coordinate of an atom of receptor and M is the number of atoms in the PDB file of receptor. Similarly, let $u_L = [x_L, y_L, z_L]$ be the $M_L \times 3$ coordinate matrix of ligand where M_L is the number of atom in the PDB file. The stochastic coordinates of ligand or receptor are given by:

$$\begin{aligned} F_R(\mathbf{v}, \omega) &= \mathbb{E}(u_R) + \sum_{k=1}^{N_R} Z_k^R(\omega) \phi_k^R(\mathbf{v}) \\ &= \mathbb{E}(u_R) + \sum_{k=1}^{N_R} \sqrt{\lambda_k} \phi_k^R(\mathbf{v}) Z_k^R(\omega). \\ Z_k^R(\omega) &= \int_D u_R(\mathbf{v}, \omega)^T \phi_k^R(\mathbf{v}) d\mathbf{v} \end{aligned}$$

and

$$\begin{aligned} F_L(\mathbf{v}, \omega) &= \mathbb{E}(u_L) + \sum_{k=1}^{N_R} Z_k^L(\omega) \phi_k^L(\mathbf{v}) \\ &= \mathbb{E}(u_L) + \sum_{k=1}^{N_L} \sqrt{\lambda_k} \phi_k^L(\mathbf{v}) Z_K^L(\omega) \\ Z_k^L(\omega) &= \int_D u_L(\mathbf{v}, \omega)^T \phi_k^L(\mathbf{v}) d\mathbf{v} \end{aligned}$$

where F_R and F_L are the truncated stochastic approximation of u_R and u_L , N_R and N_L are the number of realizations of receptor and ligand, the eigenvalues coefficients λ_k are monotonically decreasing with respect to k and Z_k^L 's are independent zero mean, unit variance Normal random variables, the eigenpair $(\lambda_k, \phi_k(\mathbf{v}))$ can be estimated empirically using the method of snapshots (see Appendix 5.4). Note that since the mean of atom coordinates may not be zero, so we need to subtract the mean of it first to get a centered process and then apply the K-L expansion on it.

With these stochastic coordinates, we can produce the PDB files of stochastic receptor/ligand domain, and furthermore generate the probabilistic shape conformation realizations of receptor and ligand which don't depend on the type of molecular maps since they are based on the position of atoms. Then by using docking software such as PIPER, the energies of stochastic domains can be obtained to compute statistics.

3.3 Computation of statistics

The objectives of this calculation are delineated in equations (7) and (8), which represent the mean and the second moment of energy, respectively. Common numerical methods for approximating integrals includes quadrature methods such as Simpson's method [25], Gaussian quadrature [26], and etc.

Quadrature methods aim to approximate definite integrals by assessing the function at designated points, subsequently applying weights, and summing the results. Let $f : S \rightarrow \mathbb{R}$ where $S := [a, b]^n$ and $a, b \in \mathbb{R}$

$$\int_S f(\mathbf{x}) d\mathbf{x} \approx \sum_{i=1}^n W_i f(\mathbf{z}_i) = \mathcal{R}(f(\mathbf{x}))$$

where $\{\mathbf{z}_i\}$ are the quadrature points, $\{W_i\}$ denote the corresponding weights, both are depend on the choice of quadrature rule, and $\mathcal{R}(f(\mathbf{x}))$ denotes the integration interpolant of function $f(\mathbf{x})$.

Considering the constraints of the protein energy manifold, direct evaluation of these integrals is non-trivial owing to the finite spectrum of known discrete values. Moreover, the stipulated quadrature points in these methods present additional challenges, especially when values at these locales are difficult to ascertain. It's important to note that if there's any irregularity at just one point within the range we're looking at, the accuracy of our approximation will suffer.

In figure 5 the energy profile for the electrostatic field with Karhunen Loeve approximation with respect to a 2

dimensional stochastic deformation from Piper is shown for the Trypsin protein. As observed, the profile appears to be locally smooth, but not globally. This motivates us to seek a more accurate representation of quantity of interest (equations (7) and (8)) that can capture high and low regularity components of the energy domain in a quadrature form. We now consider a representation based on radial basis functions (RBF) together with polynomial interpolation:

$$\mathcal{R}[f(\mathbf{x})] = \sum_{i=1}^p \mathbf{e}[i] m_i(\mathbf{z}) + \sum_{j=1}^{\eta} \mathbf{v}[j] \phi(\mathbf{z}, \mathbf{z}_j),$$

where the first term is the polynomial interpolation with lagrange basis $m_i(\mathbf{z})$ and weights $\mathbf{e}[i] \in \mathbb{R}, i = 1, \dots, p$, capturing the region of high regularity, and the second term is the radial basis interpolation with isotropic kernel function $\phi : \mathbb{R}^n \times \mathbb{R}^n \rightarrow \mathbb{R}$, nodes $\{\mathbf{z}_j\}_{j=1}^{\eta}$, and weight $\mathbf{v} \in \mathbb{R}^{\eta}$ capturing the region of low regularity.

Note that our manifold is stochastic, with suitable choice of weights and quadrature nodes $\omega_j \in \Omega$, the interpolation representation of equation (7) will be the following:

$$\begin{aligned} \mathbb{E}[\log(E(\alpha, \lambda, \omega) + \delta)] &\approx \mathcal{R}(\mathbb{E}[\log(E(\alpha, \lambda, \omega) + \delta)]) \\ &= \sum_{i=1}^p \mathbf{e}[i] m_i(\omega) + \sum_{j=1}^{\eta} \mathbf{v}[j] \phi(\omega, \omega_j) \end{aligned}$$

We introduce a quadrature scheme that employs both polynomial and radial basis functions with a Gaussian measure (in prepared). By capitalizing on the symmetry of the Gaussian measure and the centrality of quadrature points, this approach offers high accuracy at each point—even in instances of low smoothness.

4 EXPERIMENTS AND RESULTS

We test the effects of solvent uncertainty on the predicted docking site of bovine beta trypsin (chain E, Receptor) with the CMTI-I trypsin inhibitor (chain I, Ligand) from squash. Initially we run the rigid body docking code Piper [27] and the 70,000 rotations α (and corresponding translations λ) are ordered from lowest energy (best fit) to highest (worst fit). One hundred realizations of the receptor are generated using Scalable Molecular Dynamics NAMD [28] software. From these realizations an optimal truncated Karhunen-Loève (KL) [29–31] stochastic model of the receptor domain is formed:

$$\mathcal{A}(\mathbf{x}, \omega) \approx \mathbb{E}[\mathcal{A}(\mathbf{x}, \omega)] + \sum_{n=1}^{N_A} \sqrt{\mu_n} \phi_n(\mathbf{x}) Y_n(\omega). \quad (9)$$

It is assumed that the random field of the receptor domain $\mathcal{A}(\mathbf{x}, \omega)$ is a Gaussian process. The eigenpair $(\mu_n, \phi_n(\mathbf{x}))$ can be estimated empirically using the method of snapshots [32]. The eigenvalue coefficients $\mu_n \in \mathbb{R}$ are monotonically decreasing with respect to n and Y_n are independent zero mean, unit variance Normal random variables. For this experiment N_A is set to 2.

In **Figure 6**, $\mathbb{E}[\log(E(\alpha, \lambda, \omega) + \delta)]$ is plotted (blue line) and the orange line corresponds to $\text{SD}[\log(E(\alpha, \lambda, \omega))]$. The first 100 sorted rotations are plotted in **Figure 6(a)** and

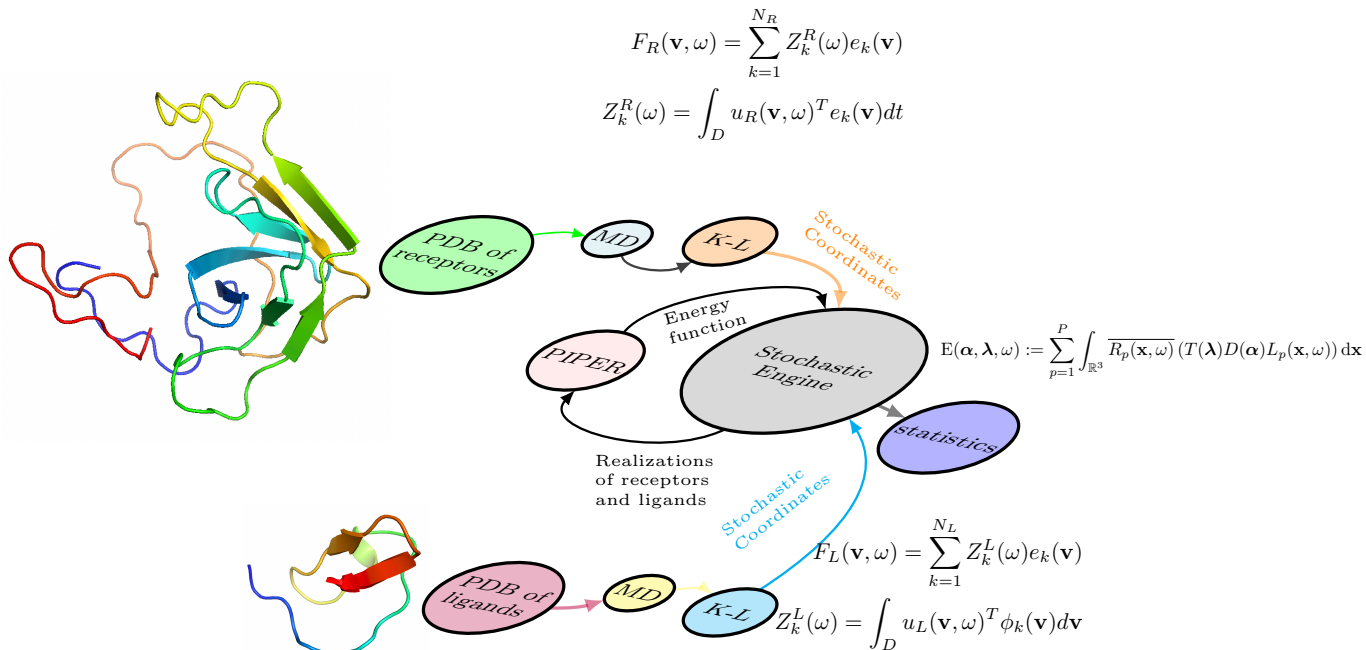


Figure 4: The flow diagram of the process of constructing stochastic framework for molecular dynamic manifold. Step 1: Obtain realizations of receptor/ligand by inputting PDB files into molecular dynamic software such as NAMD, Step 2: Apply Karhunen-Loeve expansion to generate stochastic 3-d coordinates, Step 3: Input stochastic coordinates into Stochastic Engine to generate realizations of stochastic receptor/ligand manifolds, Step 4: Use rigid protein docking program such as PIPER to evaluate interaction energies for the stochastic molecular conformation, Step 5: Compute statistics (mean and standard deviation) to look for the optimal docking site.

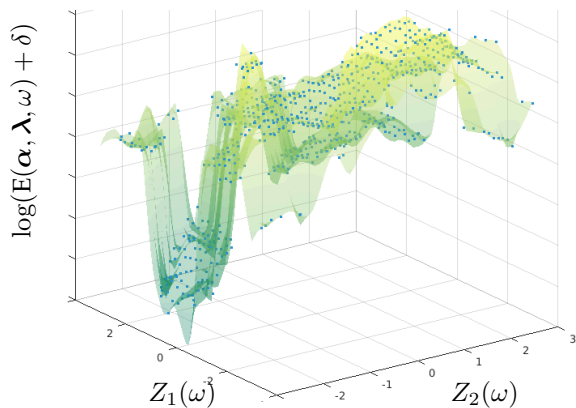


Figure 5: Energy profile from PIPER with respect to 2 dimensional stochastic deformation for Trypsin. As the figure shows, there is a relatively sharp discontinuity on the energy manifold, which prompts us to look for a more feasible method compared to traditional Gaussian quadrature methods to deal with the daunting computation task with reasonable accuracy and cost.

sorted rotations from 69,050 to 60,150 in **Figure 6(b)**. Notice that the first 100 rotations have in general a smaller mean and significantly smaller SD. The same pattern was observed for all the sorted rotations. Thus under receptor stochastic deformation the rigid body docking site predictions have low uncertainty and are consistent with the actual docking site. Low uncertainty also shows that this binding

site is robust towards stochastic domain deformations of the receptor.

When $N_A = 3$, for the same docking sites, we found that the rigid docking site predictions for the first 100 sorted rotations are much bumpier and more unstable compared to the result from two-dimensional model. The reason may be that the collision and fluctuation are much stronger in the three-dimensional protein dynamic manifold. To reduce the noise, we scale the remainder of subtracting mean from data. **Figure 7** shows that after scaling, the rigid docking site predictions under 3-dimensional stochastic deformation have low uncertainty, which is the same as the case of 2-dimensional stochastic deformation, but as rotation increases (**figure 7 (c)**), both mean and standard deviation become more oscillating. Another feasible approach might be obtaining realizations of receptors and ligand in three-dimensional with oscillation reduced at the very first step in **figure 4**. We shall investigate the predictions for rigid docking site in three or higher dimensions in more details in a future publication.

5 DISCUSSION

As we have discussed in the previous sections, the assumption of normality only changes the probability measure of stochastic manifold, the covariance structure of the molecular manifold will still be preserved. Another highlight of this model is that it does not depend on which ligand and receptor map to be used since it is based on the geometry of molecular manifold. The result for three-dimensional stochastic receptor deformations is consistent with rigid

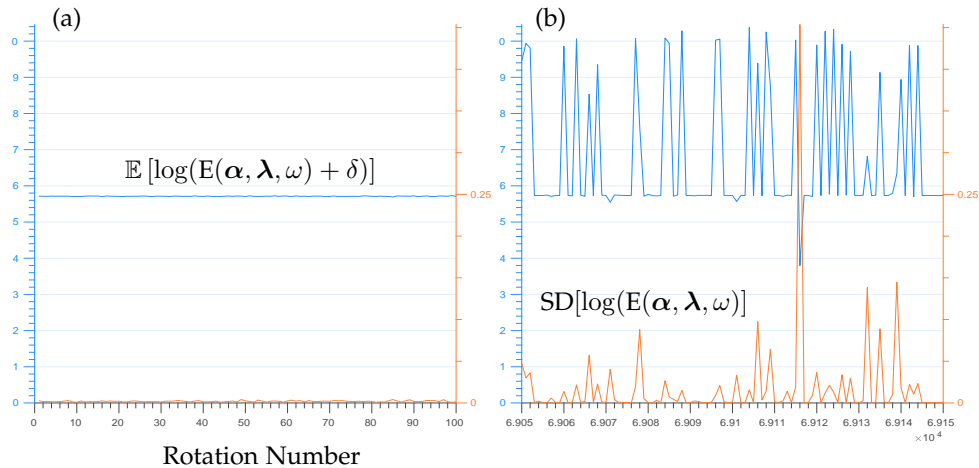


Figure 6: Trypsin energy manifold uncertainty measures with respect to 2-dimensional stochastic receptor deformations. The blue line is the mean and orange the SD. (a) First 100 top sorted rotations. Note flatness of the curve; in general mean and SD are more optimal. (b) Sorted rotations from 69,050 to 69,150.

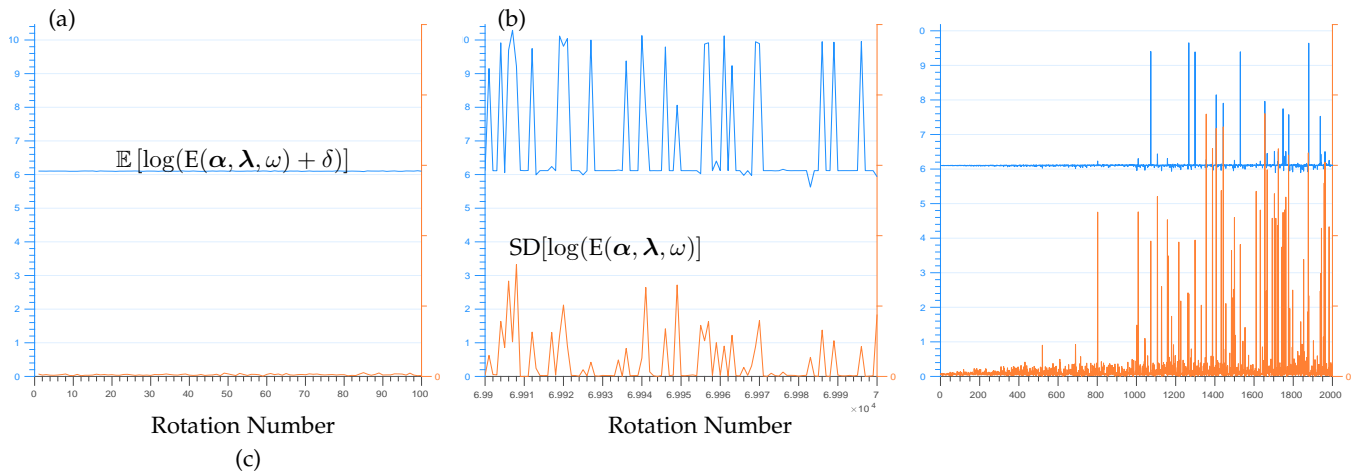


Figure 7: Trypsin energy manifold uncertainty measures with respect to 3-dimensional stochastic receptor deformations ($N_A = 3$), we multiply the random factor of KL expansion by 0.8 to reduce noise. The blue line is the mean and orange the SD. (a) First 100 top sorted rotations. Same as 2 dimensions, the curve is very flat. (b) last 100 sorted rotations. (c) First 2000 top sorted rotations.

body docking site predictions. The first one hundred top sorted rotations have much smaller uncertainty than others. However, this model provides a different ranking from rigid docking site predictions, it ranks some non-best rotation much higher. There are three main sources of errors in this framework: model error, truncation error, and integration error. As mentioned above, we assumed that the stochastic receptor manifold is a realization of a Gaussian process, wrong probability measure may lead to a model error since in most cases such random manifold does not follow a Gaussian distribution. Truncation error arises because we summarize our stochastic manifold as a three-dimensional space ($N_A = 3$), which only accounts for about 32% of the full space. To reduce truncation error and integration error, number of dimensions has to be increased, but for dimensions higher than 3, calculation will become very expensive. Full stochastic optimization could be done when an accurate numerical method is applied for high dimensional model,

which will be left for further study in the future. Because of the inaccuracy caused by high dimensions, we are unlikely to obtain the actual optimal docking site, instead we can still use this framework to determine whether a rotational and translational configuration can be considered as a good docking site with small mean and small variance of energy, following an uncertainty decision tree process.

ACKNOWLEDGMENTS

Research reported in this technical report was supported in part by the National Institute of General Medical Sciences (NIGMS) of the National Institutes of Health under award number 1R01GM131409-03 and the National Science Foundation under Grant No. 1736392.

APPENDIX

We first state the Mercer's Theorem, which is important to prove that the theorems and propositions.

Theorem 2 (Mercer's Theorem). *Suppose K is a symmetric positive definite kernel. Then there is a complete orthonormal basis $\{\phi_i\}_{i \in \mathbb{N}}$ of $L_2(D)$ consisting of eigenfunctions of $T_K : L^2(D) \rightarrow L^2(D) : f \rightarrow T_K = \int_D K(\mathbf{s}, \cdot) f(\mathbf{s}) d\mathbf{s}$, such that the corresponding sequence of eigenvalues $\{\lambda_i\}_i$ is nonnegative. Then K has the representation:*

$$K(\mathbf{s}, \mathbf{v}) = \sum_{j=1}^{\infty} \lambda_j \phi_j(\mathbf{s}) \phi_j(\mathbf{v})^T. \quad (\text{A.1})$$

Proof. see page 4-6 in [33] \square

Proof of Multivariate Karhunen Loeve Theorem (Theorem 1)

The main idea of this proof is to show that the mean squared error of truncated Karhunen-Loeve expansion converges to 0, that is equivalent to the truncated Karhunen-Loeve expansion converges to stochastic vector process $u(\mathbf{v}, \omega)$ in L_2 .

Let $Z_k(\omega) = \int_D u(\mathbf{v}, \omega)^T \phi_k(\mathbf{v}) d\mathbf{v}$, we claim that the Z_k are uncorrelated with mean zero and variance λ_k . First, we have that

$$\begin{aligned} \mathbb{E}[Z_k(\omega)] &= \mathbb{E} \left[\int_D u(\mathbf{v}, \omega) \phi_k(\mathbf{v}) d\mathbf{v} \right] \\ &= \int_D \mathbb{E}[u(\mathbf{v}, \omega)] \phi_k(\mathbf{v}) d\mathbf{v} \\ &= 0. \end{aligned}$$

Furthermore, $\mathbb{E}[Z_i(\omega) Z_j(\omega)]$

$$\begin{aligned} &= \mathbb{E} \left[\int_D \int_D \phi_i(\mathbf{v})^T u(\mathbf{v}, \omega) u(\mathbf{v}', \omega)^T \phi_j(\mathbf{v}') d\mathbf{v} d\mathbf{v}' \right] \\ &= \int_D \int_D \phi_i(\mathbf{v})^T \mathbb{E}[(u(\mathbf{v}, \omega) u(\mathbf{v}', \omega)^T) \phi_j(\mathbf{v}')] d\mathbf{v} d\mathbf{v}' \\ &= \int_D \int_D \phi_i(\mathbf{v})^T R(\mathbf{v}, \mathbf{v}') \phi_j(\mathbf{v}') d\mathbf{v} d\mathbf{v}' \\ &= \int_D \phi_i(\mathbf{v})^T \lambda_j \phi_j(\mathbf{v}) d\mathbf{v} \\ &= \delta_{ij} \lambda_j \end{aligned}$$

The equations above come from the fact that ϕ_k 's are orthonormal eigenfunctions of the operator T_{R_u} . Then, calculate the mean squared error of truncated Karhunen-Loeve expansion, we obtain an expression below with three terms:

$$\mathbb{E} \left\{ \left\| u(\mathbf{v}, \omega) - \sum_{k=1}^{\ell} (u(\mathbf{v}, \omega), \phi_k)_{L^2(D)} \phi_k \right\|_{L^2(D)}^2 \right\} \quad (\text{A.2})$$

$$= \mathbb{E} \left\{ (u(\mathbf{v}, \omega), u(\mathbf{v}, \omega))_{L^2(D)} \right\} \quad (\text{A.3})$$

$$- \mathbb{E} \left\{ \left(u(\mathbf{v}, \omega), \sum_{k=1}^{\ell} (u(\mathbf{v}, \omega), \phi_k)_{L^2(D)} \phi_k \right)_{L^2(D)} \right\} \quad (\text{A.4})$$

$$+ \mathbb{E} \left\{ \left(\sum_{k=1}^{\ell} (u(\mathbf{v}, \omega), \phi_k)_{L^2(D)} \phi_k \right)_{L^2(D)} \right\},$$

$$\sum_{k=1}^{\ell} (u(\mathbf{v}, \omega), \phi_k)_{L^2(D)} \phi_k \Big|_{L^2(D)} \Big\} \quad (\text{A.5})$$

Organizing these terms one by one we have that

$$(\text{A.3}) = \mathbb{E} \left[\left(\int_D u(\mathbf{v}, \omega)^T u(\mathbf{v}, \omega) d\mathbf{v} \right) \right] = \text{Trace}(R_u(\mathbf{v}, \mathbf{v})),$$

$$\begin{aligned} (\text{A.4}) &= 2\mathbb{E} \left[\sum_{k=1}^{\ell} \int_D \phi_k(\mathbf{v})^T u(\mathbf{v}, \omega) (u(\mathbf{v}, \omega), \phi_k)_{L^2(D)} d\mathbf{v} \right] \\ &= 2 \sum_{k=1}^{\ell} \int_D \int_D \phi_k(\mathbf{v})^T R(\mathbf{v}, \mathbf{v}') \phi_k(\mathbf{v}') d\mathbf{v}' d\mathbf{v} \\ &= 2 \sum_{k=1}^{\ell} \int_D \phi_k(\mathbf{v})^T \lambda_k \phi_k(\mathbf{v}) d\mathbf{v} \\ &= 2 \sum_{k=1}^{\ell} \lambda_k, \end{aligned}$$

and

$$\begin{aligned} (\text{A.5}) &= \sum_{k=1}^{\ell} \int_D \int_D \phi_k(\mathbf{v})^T \mathbb{E}[(u(\mathbf{v}, \omega) u(\mathbf{v}', \omega)^T)] \\ &\quad \phi_k(\mathbf{v}') d\mathbf{v}' d\mathbf{v} \\ &= \sum_{k=1}^{\ell} \int_D \lambda_k \phi_k(\mathbf{v})^T \phi_k(\mathbf{v}) d\mathbf{v} \\ &= \sum_{k=1}^{\ell} \lambda_k \end{aligned}$$

Hence,

$$\begin{aligned} &\mathbb{E} \left\{ \left\| u(\mathbf{v}) - \sum_{k=1}^{\ell} ((u(\mathbf{v}), \phi_k)_{L^2(D)} \phi_k) \right\|_{L^2(D)}^2 \right\} \\ &= (\text{A.3}) - (\text{A.4}) + (\text{A.5}) \\ &= \text{Trace}(R_u(\mathbf{v}, \mathbf{v})) - \sum_{k=1}^{\ell} \lambda_k \\ &= \text{Trace}(R_u(\mathbf{v}, \mathbf{v})) - \text{Trace} \left(\sum_{k=1}^{\ell} \lambda_k \phi_k \phi_k^T \right). \quad (\text{A.6}) \end{aligned}$$

and the final expression in equation (A.6) goes to zero as $\ell \rightarrow \infty$ by the Mercer's theorem.

Proof of Proposition 1

Suppose we have a centered Gaussian random field $u(\mathbf{v}) = (u_1(\mathbf{v}), u_2(\mathbf{v}), \dots, u_n(\mathbf{v}))^T \in L^2(\Omega)$, where $\Omega = [a_1, b_1] \times [a_2, b_2] \times \dots \times [a_n, b_n] \in \mathbb{R}^n$, each $[a_i, b_i]$ is a closed interval in \mathbb{R} for all $1 \leq i \leq n$. Let $(\cdot, \cdot)_{L^2(\Omega)}$ be the inner product defined by $(f, g)_{L^2(\Omega)} = \int_{\Omega} f^T g d\mathbf{x}$

Let

$$Z_k(\mathbf{v}) = \int_{\Omega} u(\mathbf{v})^T \phi_k(\mathbf{v}) d\mathbf{t} = \int_{\Omega} \sum_{i=1}^n u_i(\mathbf{v}) \phi_{k,i}(\mathbf{v}) d\mathbf{v}$$

Partition each interval $[a_i, b_i]$ into a finite family I_i of m_i non-overlapping closed subintervals. Then the finite family of subrectangles C given by $C = I_1 \times I_2 \times \dots \times I_n$, are in total we have $m = \prod_{i=1}^n m_i$ small rectangles C_i and $\Omega = \bigcup_{i=1}^m C_i$. Then $Z_k(\mathbf{v}) = \lim_{|\Delta| \rightarrow 0} \sum_{j=1}^m \sum_{i=1}^n u_i(\mathbf{v}_j) \phi_{k,i}(\mathbf{v}_j) m(C_j)$ where $\mathbf{v}_j \in C_j$, $m(C_j)$ is the measure of C_j , and Δ is the largest partition cube. Let $d_{i,j} = \phi_{k,i}(\mathbf{v}_j) m(C_j)$, and

$$R^k(\Delta) = \sum_{j=1}^m \sum_{i=1}^n u_i(\mathbf{v}_j) \phi_{k,i}(\mathbf{v}_j) m(C_j) = D \cdot \mathbf{U}^T$$

where

$$D = (d_{1,1}, d_{1,2}, \dots, d_{1,m}, d_{2,1}, \dots, d_{2,m}, \dots, d_{n,1}, \dots, d_{n,m})$$

and

$$\mathbf{U} = (u_1(\mathbf{v}_1), u_1(\mathbf{v}_2), \dots, u_1(\mathbf{v}_m), \\ u_2(\mathbf{v}_1), u_2(\mathbf{v}_2), \dots, u_2(\mathbf{v}_m), \\ \dots, u_n(\mathbf{v}_1), u_n(\mathbf{v}_2), \dots, u_n(\mathbf{v}_m))$$

Since $u(\mathbf{v})$ is a Gaussian random field, $u_i(\mathbf{v}_j)$ is also Gaussian. And since linear transformation preserves the Gaussian property of random variables, $R^k(\Delta)$ is also a zero mean Gaussian random variable.

$$\begin{aligned} \text{Var}(R^k(\Delta)) &= \mathbb{E}[(R^k(\Delta))^2] \\ &= \mathbb{E}\left[\sum_{j=1}^m (\phi^k(\mathbf{v}_j))^T uu^T \phi^k(\mathbf{v}_j) m(C_j)^2\right] \\ &= \sum_{j=1}^m (\phi^k(\mathbf{v}_j))^T \mathbb{E}[uu^T] \phi^k(\mathbf{v}_j) m(C_j)^2 \\ &= \sum_{j=1}^m (\phi^k(\mathbf{v}_j))^T K(\mathbf{v}_j, \mathbf{v}_j) \phi^k(\mathbf{v}_j) m(C_j)^2 \end{aligned}$$

$$\begin{aligned} \lim_{|\Delta| \rightarrow 0} \text{Var}(R^k(\Delta)) &= \int_{\Omega} \phi^k(\mathbf{v})^T K(\mathbf{v}, \mathbf{v}) \phi^k(\mathbf{v}) d\mathbf{v} \\ &= \phi^k(\mathbf{v})^T \lambda_k \phi^k(\mathbf{v}) \\ &= \lambda_k \end{aligned}$$

By computing the characteristic function of $R^k(\Delta)$ and taking a limit as $|\Delta| \rightarrow 0$, we get:

$$\begin{aligned} \lim_{|\Delta| \rightarrow 0} \mathbb{E}\left[e^{itR^k(\Delta)}\right] &= \lim_{|\Delta| \rightarrow 0} e^{it\mu - \frac{1}{2}\text{Var}(R^k(\Delta))t^2} \\ &= \lim_{|\Delta| \rightarrow 0} e^{\frac{1}{2}\text{Var}(R^k(\Delta))t^2} \\ &= e^{\frac{1}{2}\lambda_k t^2} \end{aligned}$$

Thus $Z_k \sim \mathcal{N}(0, \lambda_k)$.

Proof of Proposition 2

See Theorem 2.7 in [31]

Method of snapshots

To apply the Karhuen-Loeve expansion to the stochastic

molecular domain, we need to solve the equation (3) to get eigenfunctions $\phi_k(\mathbf{v})$. The method of snapshots by Sirovich reduces this infinite-dimensional problem of computing the eigenfunctions $\phi_k(\mathbf{v})$ to an eigenvalue decomposition problem of a finite matrix by taking samples $u(\mathbf{v}, t_k)$ at different discrete times t_k . Assume that $u(\mathbf{v})$ is an ergodic process, that is, the time average is equal to the ensemble average, the correlation can be reduced to:

$$R_u(\mathbf{s}, \mathbf{v}) = \lim_{M \rightarrow \infty} \frac{1}{M} \sum_{i=1}^M u^i(\mathbf{v}) u^i(\mathbf{s})^T$$

With finite number of samples (snapshots), $R_u(\mathbf{s}, \mathbf{v})$ can be approximated as the following:

$$R_u(\mathbf{s}, \mathbf{v}) \approx \frac{1}{M} \sum_{i=1}^M u^i(\mathbf{v}) u^i(\mathbf{s})^T \quad (\text{A.7})$$

By substituting the equation (A.7), for each k , the equation (3) becomes:

$$\frac{1}{M} \sum_{i=1}^M u^i(\mathbf{v}) \int_D u^i(\mathbf{s})^T \tilde{\phi}_k(\mathbf{s}) d\mathbf{s} = \lambda_k \tilde{\phi}_k(\mathbf{v})$$

where $u^i(\mathbf{v}) = (u_1^i(\mathbf{v}), u_2^i(\mathbf{v}), u_3^i(\mathbf{v}), \dots, u_l^i(\mathbf{v}))^T$ for $i = 1, 2, \dots, M$, and $\tilde{\phi}_k$ is the corresponding eigenfunction to the approximation of the covariance matrix function.

Define $a_{i,k} = \int_D u^i(\mathbf{s})^T \tilde{\phi}_k(\mathbf{s}) d\mathbf{s}$, then

$$\frac{1}{M} \sum_{i=1}^M a_{i,k} u^i(\mathbf{v}) = \lambda_k \tilde{\phi}_k(\mathbf{v}) \quad (\text{A.8})$$

Multiplying both sides by $u^j(\mathbf{v})^T$ and integrating over D gives:

$$\frac{1}{M} \sum_{i=1}^M a_{i,k} \int_D u^j(\mathbf{v})^T u^i(\mathbf{v}) d\mathbf{v} = \lambda_k \int_D u^j(\mathbf{v})^T \tilde{\phi}_k(\mathbf{v}) d\mathbf{v}$$

Define

$$\begin{aligned} C_{ji} &= \frac{1}{M} \int_D u^j(\mathbf{v})^T u^i(\mathbf{v}) d\mathbf{v} \\ &= \sum_{r=1}^l \frac{1}{M} \int_D u_r^j(\mathbf{v})^T u_r^i(\mathbf{v}) d\mathbf{v} \end{aligned}$$

for $i, j = 1, \dots, M$.

Then the equation (A.8) becomes:

$$\sum_{i=1}^M C_{ji} a_{i,k} = \lambda_k a_{j,k}$$

that is

$$\begin{bmatrix} C_{11} & \dots & C_{1M} \\ \vdots & & \vdots \\ C_{M1} & \dots & C_{MM} \end{bmatrix} \begin{bmatrix} a_{1,k} \\ \vdots \\ a_{M,k} \end{bmatrix} = \lambda_k \begin{bmatrix} a_{1,k} \\ \vdots \\ a_{M,k} \end{bmatrix} \quad (\text{A.9})$$

where

$$\begin{bmatrix} C_{11} & \cdots & C_{1M} \\ \vdots & & \vdots \\ C_{M1} & \cdots & C_{MM} \end{bmatrix} = \sum_{r=1}^l u_r^T u_r$$

By now, we have transferred the problem in the equation (3) to the problem of finding eigenvalues and eigenvectors of a $M \times M$ matrix showed in the equation (A.9). Most of the time the latter is much easier to compute than the former since the number of samples M is usually much smaller than the length of $u(\mathbf{v})$. And as observed, the approximation of orthonormal eigenfunctions are of the form:

$$\tilde{\phi}_k(\mathbf{v}) = \frac{1}{\lambda_k M} \sum_{i=1}^M a_{i,k} u^i(\mathbf{v})$$

REFERENCES

- [1] K. Dima, B. Ryan, C. S. R, and V. Sandor, "Piper: An fft-based protein docking program with pairwise potentials," *Proteins, structure, function, and bioinformatics*, vol. 65, no. 2, pp. 392–406, 2006.
- [2] B. G. Pierce, K. Wiehe, H. Hwang, B.-H. Kim, T. Vreven, and Z. Weng, "Zdock server: interactive docking prediction of protein-protein complexes and symmetric multimers," *Bioinformatics (Oxford, England)*, vol. 30, no. 12, p. 1771–1773, June 2014. [Online]. Available: <https://europepmc.org/articles/PMC4058926>
- [3] D. Padhorny, A. Kazennov, B. S. Zerbe, K. A. Porter, B. Xia, S. E. Mottarella, Y. Kholodov, D. W. Ritchie, and D. Kozakov, "Protein-protein docking by fast generalized fourier transforms on 5d rotational manifolds," *Proceedings of the National Academy of Sciences of the United States of America*, vol. 113, pp. 4286–4293, 2016.
- [4] C. Yang, E. A. Chen, and Y. Zhang, "Protein–ligand docking in the machine-learning era," *Molecules*, vol. 27, no. 14, 2022. [Online]. Available: <https://www.mdpi.com/1420-3049/27/14/4568>
- [5] M. Totrov and R. Abagyan, "Flexible ligand docking to multiple receptor conformations: a practical alternative," *Current Opinion in Structural Biology*, vol. 18, no. 2, pp. 178–184, 2008. [Online]. Available: <https://doi.org/10.1016/j.sbi.2008.01.004>
- [6] S.-Y. Huang and X. Zou, "Advances and challenges in protein-ligand docking," *International Journal of Molecular Sciences*, vol. 11, no. 8, pp. 3016–3034, 2010. [Online]. Available: <https://www.mdpi.com/1422-0067/11/8/3016>
- [7] N. Andrusier, E. Mashiach, R. Nussinov, and H. J. Wolfson, "Principles of flexible protein–protein docking," *Proteins: Structure, Function, and Bioinformatics*, vol. 73, no. 2, pp. 271–289. [Online]. Available: <https://onlinelibrary.wiley.com/doi/abs/10.1002/prot.22170>
- [8] S. M. Gabb HA, Jackson RM, "Modelling protein docking using shape complementarity, electrostatics and biochemical information," *Journal of molecular biology*, vol. 272, no. 1, pp. 106–120, 1997.
- [9] Z. W. Rong Chen, Li Li, "Zdock: An initial-stage protein-docking algorithm," *Proteins, structure, function, and bioinformatics*, vol. 52, no. 1, pp. 80–87, 2003.
- [10] J. Mintseris, B. Pierce, K. Wiehe, R. Anderson, R. Chen, and Z. Weng, "Integrating statistical pair potentials into protein complex prediction," *Proteins, structure, function, and bioinformatics*, vol. 69, no. 3, pp. 511–520, 2007.
- [11] H. M. Berman, J. Westbrook, Z. Feng, G. Gilliland, T. Bhat, H. Weissig, I. Shindyalov, and P. Bourne, "The protein data bank (www.pdb.org)," *Nucleic Acids Res.*, vol. 28, pp. 235–242, 2000.
- [12] M. Allen, "Introduction to molecular dynamics simulation, lecture notes," in *Computational Soft Matter: From Synthetic Polymers to Proteins, NIC Series*, N. Attig, K. Binder, H. Grubmuller, and K. Kremer, Eds. Jülich: John von Neumann Institute for Computing, 2004, vol. 23, pp. 1–28.
- [13] A. Neumaier, "Molecular modeling of proteins and mathematical prediction of protein structure," *SIAM Rev.*, vol. 39, no. 3, pp. 407–460, 1997.
- [14] J. C. e. a. Phillips, "Scalable molecular dynamics on cpu and gpu architectures with namd," *J. Chem. Phys.*, vol. 153, no. 4, p. 44130, 2020.
- [15] M. Ceriotti, G. Bussi, and M. Parrinello, "Langevin equation with colored noise for constant-temperature molecular dynamics simulations," *Physical Review Letters*, vol. 102, no. 2, p. 020601, 2009. [Online]. Available: <http://link.aps.org/abstract/PRL/v102/e020601>
- [16] P. Hänggi and P. Jung, *Colored Noise in Dynamical Systems*. John Wiley & Sons, Inc., 2007, pp. 239–326. [Online]. Available: <http://dx.doi.org/10.1002/9780470141489.ch4>
- [17] P. Jung and P. Hänggi, "Dynamical systems: A unified colored-noise approximation," *Phys. Rev. A*, vol. 35, pp. 4464–4466, May 1987. [Online]. Available: <https://link.aps.org/doi/10.1103/PhysRevA.35.4464>
- [18] K. Xia and G. Wei, "Stochastic model for protein flexibility analysis," *Phys. Rev. E*, vol. 88, p. 062709, Dec 2013. [Online]. Available: <https://link.aps.org/doi/10.1103/PhysRevE.88.062709>
- [19] N. Baker, D. Sept, S. Joseph, M. Holst, and J. McCammon, "Electrostatics of nanosystems: application to microtubules and the ribosome," *Proceedings of the National Academy of Sciences of the United States of America*, vol. 98, no. 18, p. 10037–10041, August 2001. [Online]. Available: <https://europepmc.org/articles/PMC56910>
- [20] C. Bajaj, Z. Yu, and M. Auer, "Volumetric feature extraction and visualization of tomographic molecular imaging," *Journal of Structural Biology*, vol. 144, no. 1, pp. 132 – 143, 2003, analytical Methods and Software Tools for Macromolecular Microscopy.
- [21] C. Bajaj and Z. Yu, "Geometric and signal processing of reconstructed 3d maps of molecular complexes," in *Handbook of Computational Molecular Biology*, S. Aluru, Ed. Chapman & Hall/CRC Press, 2005.
- [22] L. Sirovich, "Turbulence and the dynamics of coherent structures. i - coherent structures. ii - symmetries and transformations. iii - dynamics and scaling," *Quarterly of Applied Mathematics*, vol. 45, 10 1987.
- [23] J. E. Castrillon-Candas, D. Liu, and M. Kon, "Stochastic coordinate transformations with applications to robust machine learning," 2022.

- [24] J. E. Castrillón-Candás, F. Nobile, and R. F. Tempone, “Analytic regularity and collocation approximation for elliptic pdes with random domain deformations,” *Comput. and math. with appl.*, vol. 71, no. 6, pp. 1173–1197, Mar. 2016.
- [25] N. Shklov, “Simpson’s rule for unequally spaced ordinates,” *The American Mathematical Monthly*, vol. 67, no. 10, pp. 1022–1023, 1960. [Online]. Available: <http://www.jstor.org/stable/2309244>
- [26] T. Laudadio, N. Mastronardi, and P. Van Dooren, “Computing gaussian quadrature rules with high relative accuracy,” *Numerical Algorithms*, vol. 92, 06 2022.
- [27] D. Kozakov, D. R. Hall, D. Beglov, R. Brenke, S. R. Comeau, Y. Shen, K. Li, J. Zheng, P. Vakili, I. C. Paschalidis, and S. Vajda, “Achieving reliability and high accuracy in automated protein docking: Cluspro, piper, sdu, and stability analysis in capri rounds 13–19,” *Proteins: Structure, Function, and Bioinformatics*, vol. 78, no. 15, pp. 3124–3130, 2010. [Online]. Available: <http://dx.doi.org/10.1002/prot.22835>
- [28] J. C. Phillips, D. J. Hardy, J. D. C. Maia, J. E. Stone, J. V. Ribeiro, R. C. Bernardi, R. Buch, G. Fiorin, J. Hénin, W. Jiang, R. McGreevy, M. C. R. Melo, B. K. Radak, R. D. Skeel, A. Singharoy, Y. Wang, B. Roux, A. Aksimentiev, Z. Luthey-Schulten, L. V. Kalé, K. Schulten, C. Chipot, and E. Tajkhorshid, “Scalable molecular dynamics on cpu and gpu architectures with namd,” *The Journal of Chemical Physics*, vol. 153, no. 4, p. 044130, 2020. [Online]. Available: <https://doi.org/10.1063/5.0014475>
- [29] M. Loève, *Probability Theory II*, ser. Graduate text in Mathematics. 46. Springer, 1978.
- [30] H. Harbrecht, M. Peters, and M. Siebenmorgen, “Analysis of the domain mapping method for elliptic diffusion problems on random domains,” *Numerische Mathematik*, vol. 134, no. 4, pp. 823–856, 2016.
- [31] C. Schwab and R. A. Todor, “Karhunen–Loève approximation of random fields by generalized fast multipole methods,” *Journal of Computational Physics*, vol. 217, no. 1, pp. 100 – 122, 2006, uncertainty Quantification in Simulation Science.
- [32] J. E. Castrillón-Candás and K. Amaratunga, “Fast estimation of continuous karhunen-loeve eigenfunctions using wavelets,” *IEEE Transactions on Signal Processing*, vol. 50, no. 1, pp. 78–86, 2002.
- [33] J. E. Castrillon-Candas and M. Kon, “Stochastic functional analysis and multilevel vector field anomaly detection,” 2022.



Nanjie Chen received her Bachelor’s degree in Mathematics at Indiana University Bloomington in 2018. She is currently working toward the Ph.D. degree in Applied Mathematics at Boston University from September 2020.



dimensions.

Dongliang Yu Dongliang Yu was born on April 1th, 1995, in China. He received his B.Sc. in Information and Computing Science from Zhongnan University of Economics and Law, China, in 2017. Pursuing further education, he completed his M.Sc. in Statistics at Department of Mathematics and Statistics, Boston University in 2020 and then went to Department of Mathematics, Stony Brook University to continue his study in field of Math. Dongliang’s research is primarily centered on numerical integral methods in high



computational methods in macromolecular modeling programs such as CHARMM.

Dmitri Beglov obtained a PhD in Biophysics in Moscow Institute of Physics and Technology. He is a Research Assistant Professor in the department of Biomedical Engineering at Boston University. He has been trained in Computational Chemistry and algorithm development for molecular modeling. He is a developer and experienced user of protein docking programs Piper/ClusPro and computational solvent mapping program FTMap. He also has experience in design, development and implementation of



approximately 100 articles in mathematical physics, mathematics and statistics, computational biology, and computational neuroscience, including two books. His recent research and applications interests involve quantum probability and information, statistics, machine learning, computational biology, computational neuroscience, and complexity.

Mark Kon obtained Bachelor’s degrees in Mathematics, Physics, and Psychology from Cornell University, a PhD in Mathematics from MIT. He is a professor of Mathematics and Statistics at Boston University. He is affiliated with the Quantum Information Group, the Bioinformatics Program and the Computational Neuroscience Program. He has had appointments at Columbia University as Assistant and Associate Professor (Computer Science, Mathematics), as well as at Harvard and at MIT. He has published approxi-



Julio Enrique Castrillón-Candás received the MS and Ph.D. degrees in electrical engineering and computer science from the Massachusetts Institute of Technology (MIT), Cambridge. He is currently faculty in the department of Mathematics and Statistics at Boston University. His area of expertise is in Uncertainty Quantification (PDEs, non-linear stochastic networks), large scale computational statistics, functional data analysis and statistical machine learning.